Biochemical and Biophysical Research Communications 450 (2014) 1076–1082

Contents lists available at ScienceDirect

Biochemical and Biophysical Research Communications

journal homepage: www.elsevier.com/locate/ybbrc

Cysteine-rich secretory protein 3 inhibits hepatitis C virus at the initial phase of infection

Uk Lee, Young Ran Nam, Jung Sook Ye, Kyoung Jin Lee, Nari Kim, Chul Hyun Joo *

Department of Microbiology, Cell Dysfunction Research Center, University of Ulsan College of Medicine, Seoul 138-736, Republic of Korea

ARTICLE INFO

Article history:
Received 6 June 2014
Available online 27 June 2014

Keywords:
Hepatitis C virus
Cysteine-rich secretory protein 3
Xenograft
Cell adaptation
Immunocompromised mice

ABSTRACT

Hepatitis C virus (HCV) affects 2–3% of the global population. Approximately one-quarter of acute infections cause chronic hepatitis that leads to liver cirrhosis or hepatocellular carcinoma. The major obstacle of current research is the extremely narrow host tropism of HCV. A single HCV strain can replicate in the Huh7 human hepatoma cell line. Huh7 cells can be adapted under selective pressure *in vitro* to identify host factors that influence viral replication. Here, we extended this strategy to the *in vivo* condition and generated a series of cell lines by multiple rounds of adaptation in immunocompromised mice. Adaptation increased the cellular resistance to HCV infection. Microarray analyses revealed that the expression levels of several genes were associated with HCV resistance. Notably, up-regulation of the mRNA encoding cysteine-rich secretory protein 3 (CRISP3), a glycoprotein with unknown function that is secreted from multiple exocrine glands, was correlated with HCV resistance. The presence of CRISP3 in the culture medium limited HCV replication at the early phase of infection.

1. Introduction

Hepatitis C virus (HCV), a major cause of chronic viral hepatitis, affects 2.2–3.0% of the global population [1]. Approximately 25% of patients with chronic HCV infection develop liver cirrhosis leading to hepatocellular carcinoma [2]. HCV is a positive-strand enveloped RNA virus that belongs to the *Flaviviridae* genus [3]; its transmission is restricted to the parenteral route but its prevalence is sustained due to high infectivity and the occurrence of accidental/intentional intravenous punctures with contaminated syringes [1]. The existence of viral quasispecies continues to impede the development of specific inhibitors and vaccines. The error-prone polymerase and dynamic replication of HCV results in a circulating pool of genetic variants from which resistant strains arise [4]. Consequently, antiviral strategies have targeted the host rather than the virus [5], and host factors involved in HCV entry are particularly promising targets. HCV enters host cells by hijacking clathrin-mediated endocytosis [6]. A complex interplay between viral envelope glycoproteins and host factors, including scavenger receptor type B1, CD81, claudin-1, and occludin, is required for HCV entry [4]. Despite increasing knowledge of its host receptors, little is currently known about the host factors that limit HCV infection.

In vitro culture system has facilitated studies of HCV entry into hosts. When cultured in the Huh7 hepatoma cell line, the JFH-1 strain of HCV undergoes a full replication cycle from entry to viral particle release [7]. A number of Huh7 subclones have been derived using *in vitro* adaptation under selective pressure [8]. For example, the highly HCV-permissive Huh7.5 subclone was generated by culturing HCV-infected Huh7 cells in the presence of interferon [9] and has been used to screen for host factors that interfere with HCV replication [10]. Other subclones with different HCV replication competences have also been generated by the adaptation strategy [11]. Here, we extended this strategy to the *in vivo* condition and derived a series of adapted Huh7.5 cell lines from multiple rounds of xenograft implantation into immunocompromised mice. In subsequent studies, secreted cysteine-rich secretory protein 3 (CRISP3) inhibited HCV at the early phase of infection.

2. Materials and methods

2.1. Cells and viruses

Huh7.5 cells and Huh7A cells carrying HCV amplicons were obtained from Apath (Brooklyn, NY, USA). Hela, Huh7.5, 293T,

Abbreviations: HCV, hepatitis C virus; CA9, carbonic anhydrase 9; CRISP3, cysteine-rich secretory protein 3; CSTA, cystatin-A; IFITM2, interferon-induced transmembrane protein 2; KLF2, Krueppel-like factor 2; FIHC, fluorescent immunohistochemistry; MRI, magnetic resonance imaging.

* Corresponding author. Address: Department of Microbiology, University of Ulsan College of Medicine, Asanbyeongwon-gil 86, Songpa-gu, Seoul 138-736, Republic of Korea. Fax: +82 2 485 2320.

E-mail address: chjoo@amc.seoul.kr (C.H. Joo).

http://dx.doi.org/10.1016/j.bbrc.2014.06.106
0006-291X/

and all adapted cell lines were maintained at 37 °C in a 5% CO_2 incubator in DMEM supplemented with 10% FBS, 2 nM L-glutamine, 100 IU/ml penicillin, and 100 μg/ml streptomycin. The pJFH-1 plasmid containing the full HCV genome (GenBank: AB047639) was kindly provided by Takaji Wakita (Department of Virology, National Institute of Infectious Diseases, Tokyo, Japan). HCV particles were collected from supernatants of Huh7.5 cells transfected with *in vitro* transcribed JFH1 RNA from pJFH-1, as described previously [7]. Huh7.5 cells were repeatedly infected with HCV until the viral titer reached 1×10^8 particles/ml. HCV stocks were kept at −150 °C until use.

2.2. Cloning of CRISP3

The full length CRISP3 cDNA was purchased from Korea Human Gene Bank (Daejeon, Korea) and amplified using the Stratagene High Fidelity PCR kit (Agilent Technologies, Santa Clara, CA, USA) and primers (5′-CCC GCT AGC ACA TTA TTC CCA GTG CTG TTG-3′, 5′-CCC CTC GAG GGA ACA AAG AGG CTG CAG CAA-3′). The amplified products were purified using a PCR purification kit (Qiagen, Hilden, Germany) and then incubated with *Nhe*I and *Xho*I for 1 h. The digested products were gel-purified using the Qiagen Gel Extraction Kit. The pCMBB vector was also digested with the corresponding restriction enzymes and the fragments were ligated using the Quick Ligation Kit (NEB, Beverly, MA, USA). Transformation was performed using the standard heat-shock method.

2.3. Cell adaptation

BALB/C nude and SCID/beige mice were purchased from Orientbio (Seoul, Korea). The mice were anesthetized by intraperitoneal injection of a 10% mixture of zoletil–rompun (4:1) in saline (10 ml/kg body weight). For portal vein injection, the abdomen was sterilized with 70% alcohol and opened by midline incision. A 300 μl aliquot of PBS containing 1×10^6 cells was injected into the portal vein using a 31 gauge insulin syringe. Bleeding was controlled by pressure and the incision was closed by suturing. For flank epidermal injection, a large gauge needle was inserted into the epidermal layer and twisted to generate space for cell implantation. A 150 μl aliquot of PBS containing 1×10^7 cells was injected into each mouse using a 31 gauge insulin syringe. The mice were sacrificed 3 weeks after injection, at which stage tumor growth was identified by magnetic resonance imaging (MRI) (portal vein injection) or visually (flank injection). Tumors were resected, stored in PBS, and then divided into small pieces less than 1 mm^3 in size using surgical scissors. After centrifugation, the cell pellet was incubated for 8 h with shaking in DMEM containing 100 ng/ml collagenase type 3 (Worthington, NJ, USA). The isolated cells were subjected to clonal selection using conventional serial dilution culture.

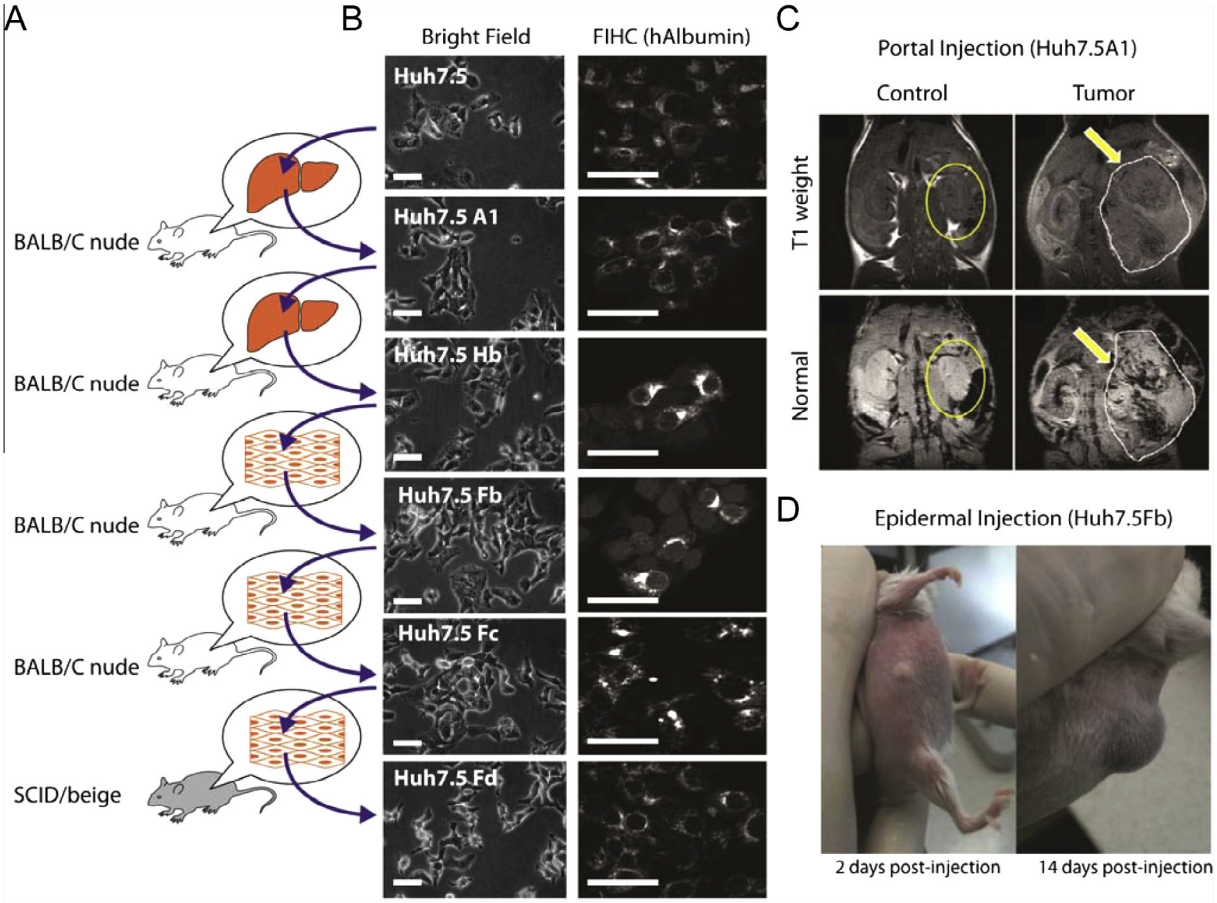

Fig. 1. Generation and characterization of adapted Huh7.5 cell lines. (A) Starting with the parental Huh7.5 cells, each adapted cell line was sequentially injected into the indicated mouse strain to generate the next adapted cell line. Adaptations comprised two rounds in the liver and two in the epidermal layers of BALB/C nude mice, and one round in the epidermal layer of SCID/beige mice. (B) Microscopy images showing the morphology of the adapted cell lines and FIHC analyses of human albumin expression. Scale bar: 50 μm. (C) MRI verification of liver tumor formation in Huh7.5A1-injected mice at 3 weeks post-injection (arrows). (D) Visual verification of tumor formation in Huh7.5Fb-injected mice at 2 and 14 days post-injection.

2.4. Microarray analysis

Total RNA was extracted from the Huh7.5 and Huh7.5Fc cells using RNeasy Plus Mini Kits (Qiagen), and then analyzed using GeneChip® Human Gene 2.0 ST Arrays (Affymetrix, Santa Clara, CA, USA) at DNAlink (Seoul, Korea).

2.5. Real-time RT-PCR

Total RNA was extracted from cells using RNeasy Plus Mini Kits (Qiagen). Quantitative real-time RT-PCR (qRT-PCR) was performed using the SYBR green II method and relative changes in cellular mRNA levels were calculated using the Pfaffl method [12]. The following sense and antisense primers were used: ACTB (5′-ATC CGC AAA GAC CTG TA-3′ and 5′-GAT CCA CAC GGA GTA CTT-3′), IFITM2 (5′-CCG ATG TCC ACC GTG ATC-3′ and 5′-TGA GCA GAA TGG TCA TGA AGA TG-3′), CRISP3 (5′-TGC TGG GCT GCT TCC AT-3′ and 5′-CGA TCC TTT GGG TTA CTG TGT-3′′), KLF2 (5′-ACG CAC CGC CAC TCA CA-3′ and 5′-CGC ACA GAT GGC ACT GGA-3′), CA9 (5′-TCG GAG CAC ACT GTG GAA G-3′ and 5′-CTC ATA TTG GAA GTA GCG GCT-3′), and CSTA (5′-CCA CTC CAG AAA TCC AGG AGA-3′ and 5′-GCC CGT CAG CTC GTC ATC-3′). Extracellular HCV RNA was extracted from 1 ml of culture media using QiAamp Viral RNA Mini Kits (Qiagen) and analyzed using the RNA Ultrasense One-Step RT-PCR System (Invitrogen, Carlsbad, CA, USA). The following TaqMan probe and primers were used to determine the absolute HCV copy numbers: sense (5′-CGG GAG AGC CAT AGT GG-3′), anti-sense (5′-AGT ACC ACA AGG CCT TTC G-3′), and probe (fluorescein-5′-CTG CGG AAC CGG TGA GTA CAC-3′-Dabcyl). The number of extracellular HCV was calculated using a standard curve.

2.6. Conditioned media

One day prior to transfection, 293T cells were seeded into 10 cm culture dishes at 30% confluence. The cells were transfected with a CRISP3-expressing or empty plasmid (20 μg/dish) using TransFectin reagent (Bio-Rad, Hercules, CA, USA). The culture medium was changed after 30 min and the conditioned media (control-CM and CRISP-CM) were collected after 12 h and stored at 4 °C (see Fig. 4A). Western blotting was performed to confirm the presence of CRIPS3 in CRISP3-CM only.

2.7. Fluorescent immunohistochemistry (FIHC)

Cells in culture plates were incubated with 10% neutral buffered formalin (BBC Biochemical, Mt. Vernon, WA, USA) for 15 min. The cells were then washed twice with PBS for 5 min, blocked with PBS containing Tween-20 (PBST) and 1% bovine serum albumin for 30 min, and then incubated with primary antibody diluted in PSBT containing 1% bovine serum albumin for 1 h. After a further three washes with PBS for 5 min, the cells were incubated with an Alexa Fluor-488-labeled secondary antibody (Invitrogen) in the dark for 1 h. All procedures were performed at room temperature. Fluorescent signals were assessed using a DM IL microscope (Leica Microsystems, Tokyo, Japan).

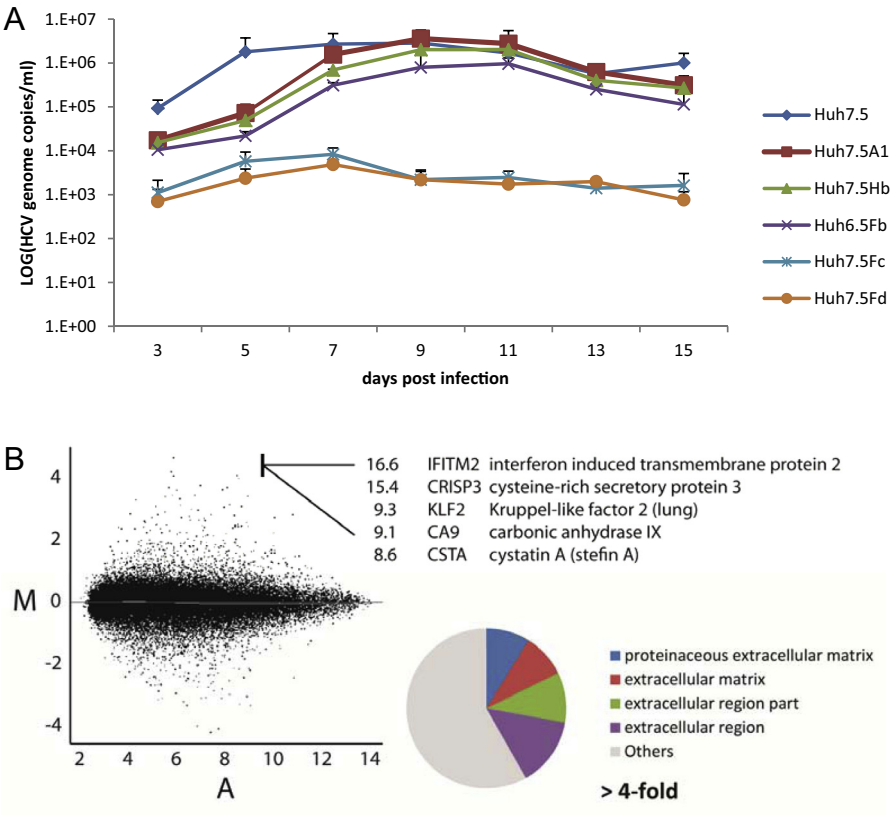

Fig. 2. Repeated Huh7.5 adaptations enhance HCV resistance. (A) HCV secretion by infected Huh7.5 parental and adapted cell lines, as determined by qRT-PCR. One day prior to HCV infection (1×10^7 particles/ml), the cells were seeded into 25T culture flasks at 30% confluence. Starting 3 days post-infection, the culture medium was replaced at 2 day intervals until the cells reached maximum confluence. The HCV RNA copy numbers were log-transformed and data are represented as the mean ± standard deviation of $n = 3$ independent experiments. (B) Microarray analysis of the Huh7.5 and Huh7.5Fc cell lines at 14 days after HCV infection. The left panel shows an MA plot and lists the top five genes that were up-regulated in the Huh7.5Fc compared with parental Huh7.5 cells. The right panel shows an ontological analysis of genes showing a greater than 4-fold change in expression.

2.8. Western blotting

Western blotting was performed using the standard method. Chemiluminescent signals were detected using an enhanced chemiluminescence solution (Pierce) and a LAS4000 digital imaging system (GE Healthcare Life Sciences, Pittsburgh, PA, USA). The anti-albumin (H-126), anti-core (C7-50), anti-CRISP3 (Y-15), and horseradish peroxidase-conjugated anti-goat IgG antibodies were purchased from Santa Cruz Biotech (Dallas, TX, USA). The anti-NS3 (1B6) and anti-actin (AC-15) antibodies were purchased from Abcam (Cambridge, MA, USA). Horseradish peroxidase-conjugated anti-mouse and rabbit IgG were purchased from Cell Signaling (Danvers, MA, USA).

3. Results

Xenograft of Huh7.5 cells into immunocompromised mice leads to the selection of cells harboring changes in gene expression that enable survival in altered external environments. Sequential xenografts were performed to generate the following series of adapted cell lines (Fig. 1A): Huh7.5A1 (portal vein injection of Huh7.5), Huh7.5Hb (portal vein injection of Huh7.5A1), Huh7.5Fb (flank epidermal injection of Huh7.5Hb), Huh7.5Fc (flank epidermal injection of Huh7.5Fb), and Huh7.5Fd (flank epidermal injection of Huh7.5Fc). The final xenograft was performed in SCID/beige mice and all other steps were performed in BALB/C nude mice. The adaptation cycle was halted at the Huh7.5Fd stage because the cells barely permitted HCV replication. The morphologies of all adapted cell lines were identical to those of the parental cells, and FIHC using a specific anti-human albumin antibody confirmed that all derived from parental Huh7.5 cells (Fig. 1B). MRI verified tumor formation in mice injected with the adapted Huh7.5A1 cells via the portal vein (Fig. 1C) and the ability of the Huh7.5Fb cells to form tumors in flank epidermal-injected mice was confirmed visually (Fig. 1D).

After infection of the adapted cells with HCV, the culture medium was changed at 2 day intervals and the amount of HCV secreted into the medium was determined by qRT-PCR on days 3–15 post-infection (Fig. 2A). HCV secretion from the parental Huh7.5 cells increased rapidly and reached a maximum around 7 days post-infection. By contrast, secretion from the Huh7.5A1, Huh7.5Hb, and Huh7.5Fb cells showed delayed kinetics, and secretion from the Huh7.5Fc and Huh7.5Fd cells was impaired markedly, suggesting that adaptation induced changes in gene expression that resulted in increased resistance to HCV.

A microarray analysis of the Huh7.5Fc and parental Huh7.5 cells revealed that approximately 45% of genes that were up-regulated more than 4-fold in the Huh7.5Fc cells compared with the parental cells were ontologically related to the extracellular environment (Fig. 2B). The five genes showing the greatest increase in expression were those encoding interferon-induced transmembrane protein 2 (IFITM2), CRISP3, Krueppel-like factor 2 (KLF2), carbonic anhydrase 9 (CA9), and cystatin-A (CSTA). The expression levels of these genes in the adapted cell lines were also determined by qRT-PCR (Fig. 3A). In agreement with the microarray data, all of the genes were expressed at markedly higher levels in the Huh 7.5Fc cells than the parental Huh7.5 cells. Notably, CRISP3 expression was correlated with the adaptation cycles. An incremental increase in CRISP3 protein levels was also confirmed by Western blotting (Fig. 3B), suggesting that the CRISP3 level is inversely correlated with HCV infectivity.

CRISP3 is a secretory protein with unknown function. To verify that secreted CRISP3 inhibits HCV, CRISP3- or control-conditioned medium (CM) was prepared from 293T cells transiently transfected with a CRISP3-expressing or empty plasmid, respectively (Fig. 4A). The presence of CRISP3 in CRISP3-CM only was confirmed by Western blotting. To determine the viral replication

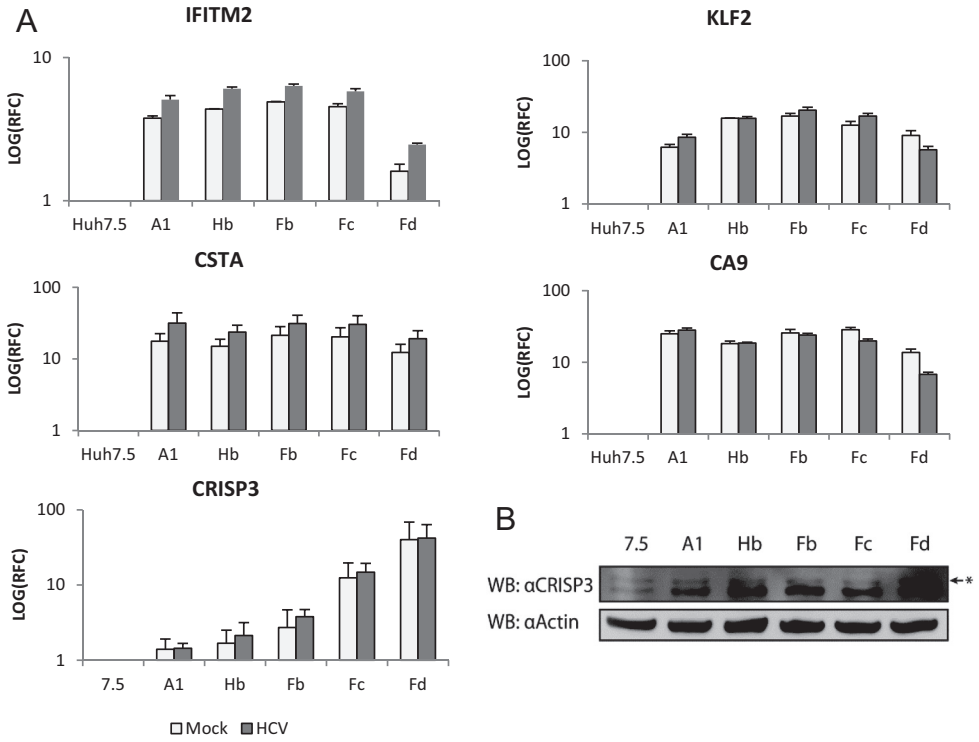

Fig. 3. CRISP3 expression is correlated with HCV resistance. (A) Expression levels of the top five genes in the parental Huh7.5 and adapted cell lines with or without HCV infection (1×10^7 particles/ml) for 14 days. Relative fold changes (RFC) were log-transformed and are represented as the mean ± standard deviation of $n = 3$ independent experiments. (B) Western blots of CRISP3 and β-actin (control) in the parental Huh7.5 and adapted cell lines. The asterisk indicates the N-glycosylated form of CRISP3.

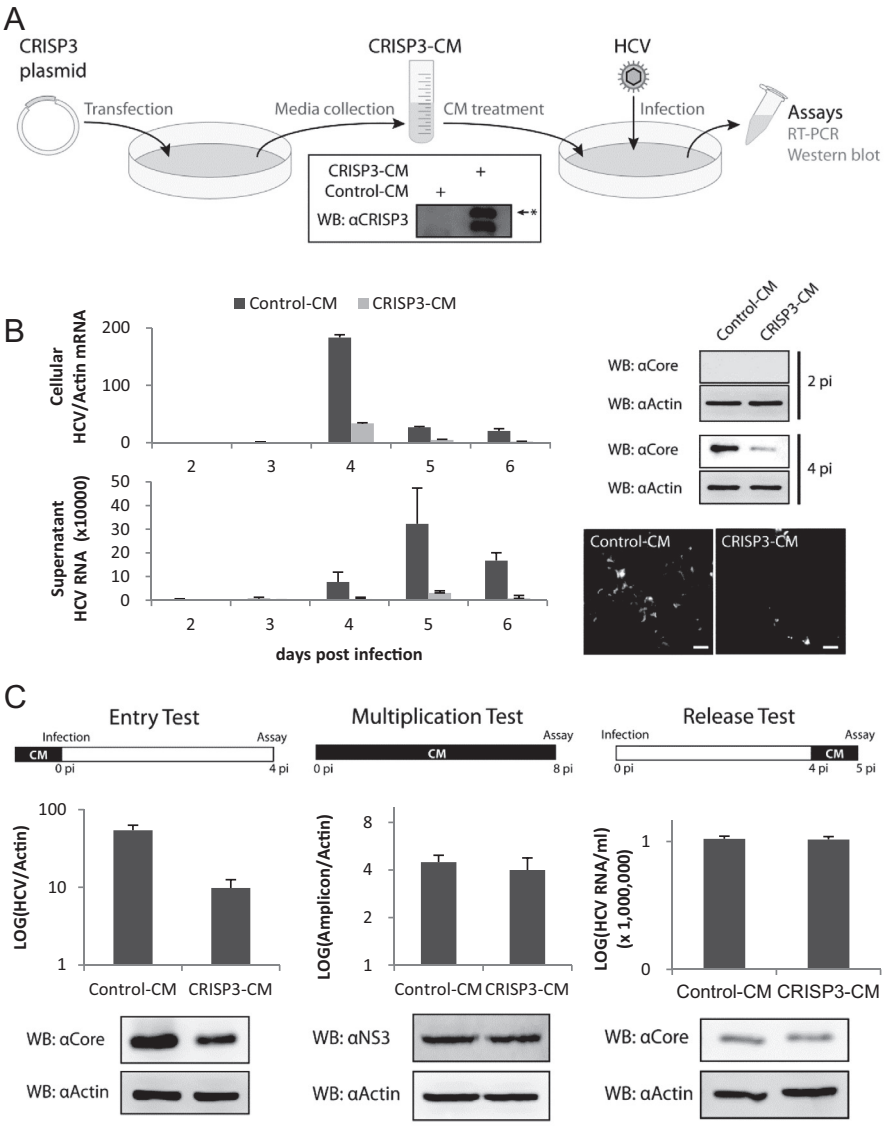

Fig. 4. Secreted CRISP3 inhibits HCV at the initial phase of infection. (A) The process for preparing conditioned media (CM). A CRISP3-expressing or empty plasmid was transfected into 293T cells and the culture media were collected after 12 h. The specific existence of CRISP3 in CRISP3-CM only was confirmed by Western blotting (inset). The asterisk indicates the N-glycosylated form of CRISP3. Huh7.5 cells were maintained in control-CM or CRISP3-CM and infected with HCV (1×10^7 particles/ml). (B) The left panels show qRT-PCR analyses of intracellular (top) and extracellular (bottom) HCV RNA levels in infected Huh7.5 cells maintained in control-CM or CRISP3-CM. Data are represented as the mean ± standard deviation of $n = 3$ independent experiments. The top right panel shows Western blot analyses of the intracellular HCV core antigen and β-actin (control) at 2 and 4 days post-infection (pi). The bottom right panel shows FIHC analyses of the anti HCV core antigen at 4 days post-infection. (C) Western blot and qRT-PCR analyses of the effects of extracellular CRISP3 on HCV infection. In the entry inhibition test, Huh7.5 cells were infected with a mixture of CM and HCV (1×10^7 particles/ml) for 1 h, and then cultured in normal medium for a further 4 days. In the multiplication test, Huh7A cells carrying HCV amplicons were maintained in control-CM or CRIPS3-CM for 8 days. In the release test, Huh7.5 cells were infected with HCV (1×10^7 particles/ml), maintained in DMEM for 4 days, and then replaced with CM for a further 24 h. In Western blot analyses, β-actin was used as a loading control. The intracellular HCV RNA expression levels were also normalized to those of β-actin and the data are represented as the mean ± standard deviation of $n = 3$ independent experiments.

kinetics, intracellular and extracellular HCV RNA levels were measured in Huh7.5 cells maintained in control-CM or CRISP3-CM (Fig. 4B, left panels). In the control-CM-maintained cells, intracellular HCV replication peaked after 4 days and HCV secretion peaked at 5 days post-infection. Although a similar pattern was observed for the CRISP3-CM-maintained cells, the HCV RNA levels were considerably lower at all-time points. Western blot and FIHC analyses of the HCV core antigen indicated that the level of virus replication at 4 days post-infection was much lower in the CRISP3-CM-maintained cells than those grown in control-CM (Fig. 4B, right panels).

Viral replication can be divided into three major steps: host cell entry, intracellular replication of progeny, and release from host cells. To determine whether CRISP3 influences viral entry into host cells, HCV was mixed with control-CM or CRISP3-CM for 3 h and Huh7.5 cells were infected with the mixtures for 1 h. The cells were then washed and the medium was replaced with simple DMEM. At 4 days post-infection, intracellular HCV RNA and core protein levels were lower in the cells infected with CRISP3-CM-incubated HCV than those infected with control-CM-incubated HCV (Fig. 4C, left panel). To assess the influence of CRISP3 on intracellular viral replication, Huh7A cells were maintained in control-CM or CRISP3-CM. Huh7A cells carry a HCV amplicon that replicates inside cells but does not produce infectious particles due to the total deletion of structural genes [13]. At 8 days post-infection, there were no differences between the intracellular HCV amplicon levels in the control-CM- and CRISP3-CM-maintained cells. Similarly, the levels of NS3 (a non-structural HCV protein) were

comparable in each cell type (Fig. 4C, middle panel). To determine the influence of CRISP3 on viral release, Huh7.5 cells were infected with HCV and maintained in simple DMEM for 4 days, followed by control-CM or CRISP3-CM for a further 24 h. Western blot analyses of intracellular HCV core protein levels and qRT-PCR analyses of HCV secretion revealed no differences between the control-CM- and CRISP3-CM-maintained cells. Taken together, these data indicate that secreted CRIPS3 inhibits HCV at the early phase of infection.

4. Discussion

Cancer cell lines have genetic instability; therefore, adaptation under selective pressure induces changes in the expression levels of genes that enable survival in altered environments. This study describes the generation of a series of adapted Huh7.5 cell lines via repeated xenografts in immunocompromised mouse. HCV replication was limited in the adapted cell lines. Furthermore, CRISP3 expression was inversely correlated with HCV replication and secreted CRISP3 inhibited HCV at the early phase of infection.

A microarray analysis revealed that IFITM2, CRISP3, KLF2, CA9, and CSTA, all of which are ontologically related to the extracellular environment, were up-regulated in the adapted cells compared with the parental cells. IFITM2 is a transmembrane protein that is induced by interferon stimulation in response to viral infection [14]. IFITM2 blocks viral entry by preventing fusion of the viral and late endosomal membranes during endocytosis [14]. KLF2 is a transcription factor that expresses receptors involved in immune cell trafficking regulation [15]. CA9 is a plasma membrane protein that regulates intracellular acidity and is related to cellular transformation [16]. CSTA is an intracellular proteinase inhibitor that controls cell–cell adhesion [17]. Although these proteins may also inhibit HCV replication, we focused on CRISP3 because it is a secretory protein with unknown function. Up-regulation of CRISP3 has been reported in some pathologic conditions, such as Sjögren's syndrome [18], oral squamous cell carcinoma [19], and prostate cancer [20].

CRISP3 belongs to a large family of proteins that are highly conserved among vertebrates [21] and contain a signature C-terminal cysteine cluster [22]. Other proteins in the family have a variety of functions and four CRISP proteins have been identified in humans to date. CRISP1, CRISP2, and CRISP4 are expressed in the sexual glands and have roles in sperm maturation and fertilization [23]. CRISP1 associates with zinc ions during sperm maturation [24]. Distantly related CRISP proteins are also found in reptile venoms [22]; injection of CRISP-containing venom into prey animals disrupts cellular homeostasis by blocking cyclic nucleotide- or voltage-gated ion channels [25]. Although its function has not yet been defined, CRISP3 is a matrix glycoprotein that is localized in a subset of peroxidase-negative granules of neutrophils, suggesting that it may be related to innate immunity [26,27]. As the most abundant white blood cell, neutrophils are the first responders to invading pathogens; hence, release of CRISP3 into the inflammation site may play a role in the defense against pathogen spreading. In support of this concept, CRISP3 is homologous to pathogen-resistant proteins of plants, which are induced in response to infection [28]. CRISP3 shows a wider exocrine distribution than other CRISP proteins, being expressed in the salivary glands, pancreas, prostate gland, epididymis, ovary, thymus, and colon [21].

Although it is beyond the scope of this work, the mechanisms by which secreted CRISP3 inhibits HCV infection are intriguing. CRISP3 may bind to the envelope of HCV and prevent its attachment to host cell receptors, or may bind to the host cell surface and interfere with the viral entry process that hijacks cellular endocytosis.

Acknowledgments

This work was supported by the National Research Foundation of Korea (NRF), an MRC grant funded by the Korea government (MSIP) (2008-0062286) and the Asan Institute for Life Sciences (2011-346).

References

[1] D. Lavanchy, The global burden of hepatitis C, Liver Int. 29 (Suppl. 1) (2009) 74–81.
[2] M.H. Heim, Innate immunity and HCV, J. Hepatol. 58 (2013) 564–574.
[3] D. Moradpour, F.C.O. Penin, C.M. Rice, Replication of hepatitis C virus, Nat. Rev. Microbiol. 5 (2007) 453–463.
[4] M.B. Zeisel, I. Fofana, S. Fafi-Kremer, T.F. Baumert, Hepatitis C virus entry into hepatocytes: molecular mechanisms and targets for antiviral therapies, J. Hepatol. 54 (2011) 566–576.
[5] P. Georgel, C. Schuster, M.B. Zeisel, F.O. Stoll-Keller, T. Berg, S. Bahram, et al., Virus-host interactions in hepatitis C virus infection: implications for molecular pathogenesis and antiviral strategies, Trends Mol. Med. 16 (2010) 277–286.
[6] E. Blanchard, S. Belouzard, L. Goueslain, T. Wakita, J. Dubuisson, C. Wychowski, et al., Hepatitis C virus entry depends on clathrin-mediated endocytosis, J. Virol. 80 (2006) 6964–6972.
[7] T. Wakita, T. Pietschmann, T. Kato, T. Date, M. Miyamoto, Z. Zhao, et al., Production of infectious hepatitis C virus in tissue culture from a cloned viral genome, Nat. Med. 11 (2005) 791–796.
[8] J.I. MacPherson, B. Sidders, S. Wieland, J. Zhong, P. Targett-Adams, V. Lohmann, et al., An integrated transcriptomic and meta-analysis of hepatoma cells reveals factors that influence susceptibility to HCV infection, PLoS One 6 (2011) e25584.
[9] K.J. Blight, J.A. McKeating, C.M. Rice, Highly permissive cell lines for subgenomic and genomic hepatitis C virus RNA replication, J. Virol. 76 (2002) 13001–13014.
[10] R. Sumpter Jr., Y.-M. Loo, E. Foy, K. Li, M. Yoneyama, T. Fujita, et al., Regulating intracellular antiviral defense and permissiveness to hepatitis C virus RNA replication through a cellular RNA helicase, RIG-I, J. Virol. 79 (2005) 2689–2699.
[11] J. Zhong, P. Gastaminza, G. Cheng, S. Kapadia, T. Kato, D.R. Burton, et al., Robust hepatitis C virus infection in vitro, Proc. Natl. Acad. Sci. 102 (2005) 9294–9299.
[12] M.W. Pfaffl, A new mathematical model for relative quantification in real-time RT–PCR, Nucleic Acids Res. 29 (2001) e45.
[13] K.J. Blight, A.A. Kolykhalov, C.M. Rice, Efficient initiation of HCV RNA replication in cell culture, Science, 2000.
[14] A.L. Brass, I.-C. Huang, Y. Benita, S.P. John, M.N. Krishnan, E.M. Feeley, et al., The IFITM proteins mediate cellular resistance to influenza A H1N1 virus, West Nile virus, and dengue virus, Cell 139 (2009) 1243–1254.
[15] M.A. Weinreich, K. Takada, C. Skon, S.L. Reiner, S.C. Jameson, K.A. Hogquist, KLF2 transcription-factor deficiency in T cells results in unrestrained cytokine production and upregulation of bystander chemokine receptors, Immunity 31 (2009) 122–130.
[16] M. Hilvo, L. Baranauskiene, A.M. Salzano, A. Scaloni, D. Matulis, A. Innocenti, et al., Biochemical characterization of CA IX, one of the most active carbonic anhydrase isozymes, J. Biol. Chem. 283 (2008) 27799–27809.
[17] D.C. Blaydon, D. Nitoiu, K.-M. Eckl, R.M. Cabral, P. Bland, I. Hausser, et al., Mutations in CSTA, encoding cystatin A, underlie exfoliative ichthyosis and reveal a role for this protease inhibitor in cell–cell adhesion, Am. J. Hum. Genet. 89 (2011) 564–571.
[18] N.I. Tapinos, M. Polihronis, G. Thyphronitis, H.M. Moutsopoulos, Characterization of the cysteine-rich secretory protein 3 gene as an early-transcribed gene with a putative role in the pathophysiology of Sjögren's syndrome, Arthritis Rheum. 46 (2002) 215–222.
[19] W.-C. Ko, K. Sugahara, T. Sakuma, C.-Y. Yen, S.-Y. Liu, G.-A. Liaw, et al., Copy number changes of CRISP3 in oral squamous cell carcinoma, Oncol. Lett. 3 (2012) 75–81.
[20] F. Kosari, Y.W. Asmann, J.C. Cheville, G. Vasmatzis, Cysteine-rich secretory protein-3: a potential biomarker for prostate cancer, Cancer Epidemiol. Biomarkers Prev. 11 (2002) 1419–1426.
[21] J. Krätzschmar, B. Haendler, U. Eberspaecher, D. Roosterman, P. Donner, W.D. Schleuning, The human cysteine-rich secretory protein (CRISP) family. Primary structure and tissue distribution of CRISP-1, CRISP-2 and CRISP-3, Eur. J. Biochem. 236 (1996) 827–836.
[22] Y. Yamazaki, F. Hyodo, T. Morita, Wide distribution of cysteine-rich secretory proteins in snake venoms: isolation and cloning of novel snake venom cysteine-rich secretory proteins, Arch. Biochem. Biophys. 412 (2003) 133–141.
[23] D.J. Cohen, D. Busso, V. Da Ros, D.A. Ellerman, J.A. Maldera, N. Goldweic, et al., Participation of cysteine-rich secretory proteins (CRISP) in mammalian sperm–egg interaction, Int. J. Dev. Biol. 52 (2008) 737–742.
[24] J.A. Maldera, G. Vasen, J.I. Ernesto, M. Weigel-Muñoz, D.J. Cohen, P.S. Cuasnicu, Evidence for the involvement of zinc in the association of CRISP1 with rat sperm during epididymal maturation, Biol. Reprod. 85 (2011) 503–510.

[25] K. Sunagar, W.E. Johnson, S.J. O'Brien, V. Vasconcelos, A. Antunes, Evolution of CRISPs associated with toxicoferan-reptilian venom and mammalian reproduction, Mol. Biol. Evol. 29 (2012) 1807–1822.
[26] L. Kjeldsen, J.B. Cowland, A.H. Johnsen, N. Borregaard, SGP28, a novel matrix glycoprotein in specific granules of human neutrophils with similarity to a human testis-specific gene product and a rodent sperm-coating glycoprotein, FEBS Lett. 380 (1996) 246–250.
[27] L. Udby, J. Calafat, O.E. Sørensen, N. Borregaard, L. Kjeldsen, Identification of human cysteine-rich secretory protein 3 (CRISP-3) as a matrix protein in a subset of peroxidase-negative granules of neutrophils and in the granules of eosinophils, J. Leukoc. Biol. 72 (2002) 462–469.
[28] P. Pfisterer, H. König, J. Hess, G. Lipowsky, B. Haendler, W.D. Schleuning, et al., CRISP-3, a protein with homology to plant defense proteins, is expressed in mouse B cells under the control of Oct2, Mol. Cell. Biol. 16 (1996) 6160–6168.